

INFRARED EMISSION FROM PHOTO-EXCITED GASEOUS BENZENE: DETECTION WITH A NEW HOME-MADE SPECTROMETER

G. Féraud¹, Y. Carpentier², T. Pino¹, Y. Longval³, E. Dartois³,
T. Chamailé¹, R. Vasquez¹, J. Vincent¹, P. Parneix¹, C. Falvo¹
and Ph. Bréchnignac¹

Abstract. The infrared fluorescence decay and the dispersed emission spectrum are presented for gaseous benzene following 193 nm laser excitation. They were measured with FIREFLY (Fluorescence in the InfraRed from Excited FLYing molecules), a new home-made spectrometer. Redshift and redtail in the CH stretch emission spectra (3.3 μm region) demonstrate that anharmonicity plays a key role when dealing with high internal energies, as it is the case in the interstellar medium.

1 Introduction

Aromatic Infrared Bands (AIBs) have been observed for the very first time by Gillett *et al.* (1973) in the mid-infrared (IR) spectral range. Since then, Polycyclic Aromatic Hydrocarbons (PAHs) have been investigated as plausible carriers for these bands (Allamandola *et al.* 1985; Joblin & Tielens 2011; Léger & Puget 1984). Thanks to satellites such as IRAS, ISO, Spitzer, Akari and earth-bound or airborne instruments (Giard *et al.* 1989; Jourdain de Muizon *et al.* 1986), numerous observations of AIBs have been reported. AIBs are mainly found at 3.3 μm , 6.2 μm , “7.7” μm , 8.6 μm , 11.3 μm and 12.7 μm in various environments, from diffuse clouds to stellar systems. Based on their position and shape, the AIBs can be separated in three main classes A, B and C (Peeters *et al.* 2002), which reveal different families of carriers with different growth scenarios and evolutionary links (Acke *et al.* 2010; Carpentier *et al.* 2012; Pino *et al.* 2008; Sloan *et al.* 2007; Carpentier *et al.* elsewhere in this volume). The important differences between the classes are in the 6.2 μm and “7.7” μm positions (redshifted from class A to C)

¹ Institut des Sciences Moléculaires d’Orsay, Université Paris-Sud 11, France

² Laboratoire de Physique des Lasers, Atomes et Molécules, Université de Lille 1, France

³ Institut d’Astrophysique Spatiale, Atomes et Molécules, Université Paris-Sud 11, France

and in the type of observed object. Ultraviolet (UV) photon absorption can lead to different competing processes such as ionisation, desorption, fragmentation and infrared emission. In this paper we will focus on the latter, also called infrared fluorescence. This long lasting phenomenon (a few seconds) challenges modelling (Basire *et al.* 2008; Cook & Saykally 1998; Puget & Léger 1989) as well as gas phase experiments (Brenner & Barker 1992; Cherchneff & Barker 1989; Cook & Saykally 1998; Cook *et al.* 1998; Shan *et al.* 1991; Williams & Leone 1995). We present the IR fluorescence decay and the dispersed emission spectrum (in the CH stretch region around $3.3 \mu\text{m}$) of benzene obtained with a new home-made spectrometer. We choose to begin with the benzene molecule in gas phase as a well-studied prototype and a building block of the PAH family.

2 Experiment

A spectrometer dedicated to measuring weak IR emission signals from photo-excited gas phase molecules, FIREFLY (Fluorescence in the InfraRed from Excited FLYing molecules), has been built (Fig. 1) as part of the Nanograins project at the Institut des Sciences Moléculaires d'Orsay (France). The instrument is at room temperature and atmospheric pressure, and is coupled to a cell containing flowing benzene (Sigma-Aldrich, purity $\geq 99\%$) from a liquid reservoir maintained under low pressure and at ambient temperature. The flow of molecules is controlled by a dosing valve. It forms an effusive flow through a 4 mm diameter hole and the residual pressure in the cell is around 0.2 mbar. An argon flow is used to protect the CaF_2 entrance window of the cell from soot formation under laser irradiation. This implies that argon pressure has to be higher than the benzene one (>1 mbar). The benzene-argon collisional rate is estimated to $1.5 \cdot 10^7 \text{ s}^{-1}$ and the benzene-benzene collisional rate $7 \cdot 10^5 \text{ s}^{-1}$.

A nanosecond ArF excimer laser beam (Neweks) photoexcites gaseous benzene at 193 nm (51800 cm^{-1}). The fluence is kept lower than 3 mJ/pulse to avoid multiphoton effects and the repetition rate is set to 100 Hz. The UV beam is directed perpendicularly to the infrared spectrometer general axis in order to avoid damages by the energetic photons. As no collection optics is used to couple the emission region with the spectrometer, only a small solid angle (≈ 0.05 steradians *i.e.*, 0.4%) of the isotropic IR emission is detected, optimized for this instrument.

The main elements of the instrument are the narrow bandpass interferential Circular Variable Filters (CVFs) replicated from the ISOCAM instrument (Cesarsky *et al.* 1996). They consist of three segments, covering the $2.45 \mu\text{m}$ (4073 cm^{-1}) to $14.5 \mu\text{m}$ (690 cm^{-1}) spectral range. In this experiment, only the $2.45 \mu\text{m}$ (4073 cm^{-1}) to $4.55 \mu\text{m}$ (2195 cm^{-1}) segment is used in order to probe the CH stretch region. They have a high transmission (75% at $3.3 \mu\text{m}$) and a moderate resolving power ($\lambda/\delta\lambda = 45$ at $3.3 \mu\text{m}$). They are fixed on a computer-controlled rotatable wheel. Specific ellipsoid mirrors have been designed to shape the IR beam to the desired dimensions. They are gold-coated without any additional protection, so that the reflection coefficient is at least 97–98% in the 2–20 μm spectral range. The first mirror focuses the beam on the filter with a

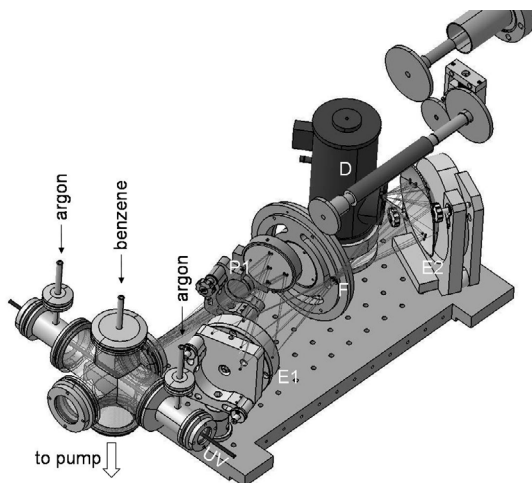


Fig. 1. Scheme of the infrared emission spectrometer. The cell with benzene and argon tubes is represented (*left*). The UV beam crosses the cell (*lower left*). The IR beam is represented by multiple grey lines. A plane mirror (P1) reflects the light on a first ellipsoid mirror (E1) which focuses the beam on the rotatable wheel containing the 2.45 μm (4073 cm^{-1}) to 4.55 μm (2195 cm^{-1}) bandpass filter (F). It diverges and a second ellipsoid mirror (E2) focuses the beam on the InSb detector (D).

rectangular cross section of $2.5 \times 7.5\text{ mm}^2$. A second mirror shapes again the beam into a $2 \times 2\text{ mm}^2$ square cross section optimized for a nitrogen cooled InSb detector (Infrared Associates). The signal is then amplified through a 1.5 Hz–20 kHz preamplifier before being digitized and recorded via a computer. The instrument was spectrally calibrated using gaseous ethanol, benzene and CO_2 absorptions with, in this case, a 873 K blackbody radiation as an IR source.

3 Results and discussion

Benzene has six CH stretching modes including two IR active ones. After electronic absorption (cross section at 193 nm $\approx 20 \cdot 10^{-18}\text{ cm}^2$ as reported by Suto *et al.* 1992), several non radiative and radiative processes occur. Successive internal conversions convert the initial electronic excitation in the S_2 state ($^1\text{B}_{1u}$) into ground state high vibrational excitation, accompanied by Intramolecular Vibrational energy Redistribution (IVR – for a review, see Nesbitt & Field 1996) and followed by the emission of IR photons forming a long-lasting cascade. Figure 2a shows the infrared fluorescence decay following 193 nm excitation at $t = 0$, with a 10^{-8} s resolution. No interferential filters are used (the wavelength range is therefore that one of the InSb detector *i.e.*, 2.5 to 5.5 μm) and the signal is averaged over 300 laser shots. The initial rise of $\approx 4\text{--}5\ \mu\text{s}$ is due to the response time of the detector and 1.5 Hz–20 kHz preamplifier. The decay fits well with a biexponential function with characteristic times of 8 μs and 135 μs . A single exponential

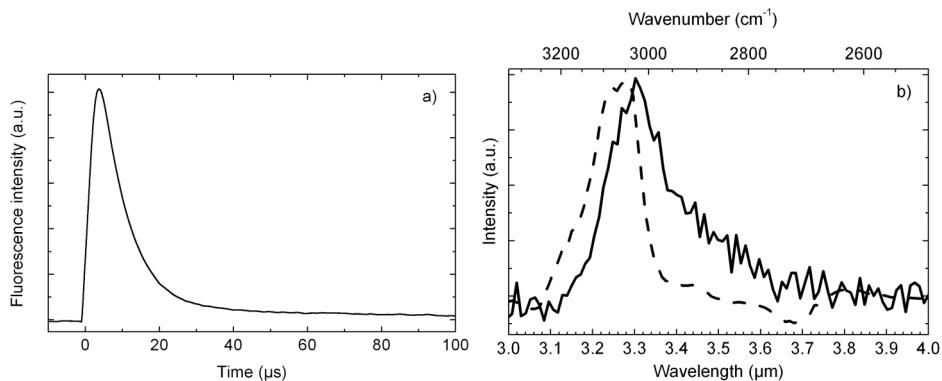


Fig. 2. a) Total fluorescence decay (CH stretch region) following 193 nm excitation for gas phase benzene. $t=0$ stands for the UV excitation. b) Dispersed IR fluorescence as a function of the wavelength (CH stretch region) following 193 nm excitation for gas phase benzene. Dashed line: benzene absorption (300 K, ≈ 90 mbar) recorded with the same spectrometer. The wavelength step is $0.01 \mu\text{m}$.

decay is not expected and the precise modeling of [Barker & Golden \(1984\)](#) and [Yerram *et al.* \(1990\)](#) is preferred and briefly discussed hereafter. Such a fit gives only access to a rough evaluation of the cooling rate. The spectrally resolved IR fluorescence in the CH stretch region is shown in Figure 2b. It was obtained by integrating the time-resolved IR signal through the $0\text{--}100 \mu\text{s}$ windows for each wavelength from $3 \mu\text{m}$ (3333 cm^{-1}) to $4 \mu\text{m}$ (2500 cm^{-1}) with a $0.01 \mu\text{m}$ step. A noticeable redtail is observed in the spectrum up to $4 \mu\text{m}$. Redshift and redtail are the signatures of anharmonicity in the ground electronic state. The presented spectrum compares very well with that of [Shan *et al.* \(1991\)](#) (infrared emission from excited benzene at 193 nm in a cell), although ours seems to be slightly wider. Benzene IR absorption at 300 K is also shown in Figure 2b (dashed line). The IR source is a 873 K blackbody radiation and FIREFLY was used with a lock-in amplifier to record the spectrum. The emission and the absorption bands differ in position, width and asymmetry. The first moment of the emission band located at 2994 cm^{-1} is 74 cm^{-1} redshifted from the first moment of the absorption band located at 3068 cm^{-1} and the width of the emission band is significantly larger than the absorption band (Fig. 2b). These differences between absorption and emission clearly show the preponderant role of the internal energy. [Williams & Leone \(1995\)](#) and [Cook *et al.* \(1998\)](#) measured the naphthalene IR emission for two different excitation energies and showed that the higher the internal energy, the stronger the redshift and redtail are, as a consequence of the anharmonicity.

IR emission cascades measured in the laboratory are faster than interstellar ones. This is mainly because the collisional quenching, only present in the experiment, opens a new competing relaxation pathway. [Barker & Golden \(1984\)](#) and [Yerram *et al.* \(1990\)](#) quantified the internal energy loss per molecular collision as a function of the internal energy by measuring IR fluorescence rates. They found

that collisions between excited benzene and unexcited benzene efficiently reduce the internal energy (by about 1500 cm^{-1} per collision at an internal energy of $40\,000\text{ cm}^{-1}$). Given our collisional rate, the order of magnitude of internal energy loss is $10\,000\text{ cm}^{-1}$ in $10\ \mu\text{s}$. Another competing pathway is the benzene dissociation. Tsai *et al.* (2000) and Kislov *et al.* (2004) measured and calculated that the values of the benzene lifetime at 193 nm are respectively 10 and 11 μs and that the branching ratio for H-loss is 99.6%. One could wonder to what extent the phenyl radical C_6H_5 contributes to the recorded emission: the CH bond clivage costs 4.9 eV (Davico *et al.* 1995), so the phenyl product internal energy is less than 1.5 eV (6.4 eV–4.9 eV); because such internal energy is somehow comparable to the CH stretch frequency (0.4 eV), radiative relaxation through that channel is not favoured. Moreover, the absolute phenyl CH stretch (3071 cm^{-1}) absorption intensity is smaller than the benzene CH stretch absorption intensity (Friderichsen *et al.* 2001; Spedding & Whiffen 1956). Therefore, no strong emission from the phenyl radical is expected. Due to collisional quenching, the benzene dissociation is less and less likely and only the competition between IR emission and collisions remains.

4 Conclusion

The IR fluorescence decay and the spectrally resolved emission spectrum are presented for gaseous benzene excited at 193 nm, highlighting a large anharmonicity. Spectroscopic differences between absorption and emission spectra underline the necessity to compare astrophysical emission data not only with laboratory absorption spectra but also with emission spectra, under conditions similar to those encountered in space. As mentioned in the introduction, benzene represents a prototype molecule, showing a broader emission spectrum than the $3.3\ \mu\text{m}$ AIB which typically has a 30 cm^{-1} FWHM. As shown for example by Shan *et al.* (1991), for increasingly larger PAHs, the emission band becomes narrower and similar to the AIBs. Due to experimental limitations, coronene is the biggest PAH measured in emission (Cook *et al.* 1996). The interstellar emitters should however not exceed a size of a few hundreds carbon atoms, in order to reach the temperatures of $\sim 1000\text{ K}$ that are required to emit at $3.3\ \mu\text{m}$. More generally, IR emission measurements are essential tools to improve our understanding of molecules. Observations, theoretical and experimental research need to continue their joined effort to shed new light on the AIB carriers.

The authors wish to thank L. Vigroux for giving them the opportunity to use the CVF filters. This work was in part supported by the French CNRS-INSU national program “Physique et Chimie du Milieu Interstellaire” (PCMI) and by the French Agence Nationale de la Recherche under the project grant ANR-10-BLAN-0501-GASPARIM.

References

- Acke, B., Bouwman, J., Juhsz, A., *et al.*, 2010, ApJ, 718, 558
Allamandola, L.J., Tielens, A.G.G.M., & Barker, J.R., 1985, Astrophys. J. Lett., 290, L25

- Barker, J.R., & Golden, R.E., 1984, *J. Phys. Chem.*, 88, 1012
- Basire, M., Parneix, P., & Calvo, F., 2008, *J. Chem. Phys.*, 129, 081101
- Brenner, J., & Barker, J.R., 1992, *ApJ*, 388, L39
- Carpentier, Y., Féraud, G., Dartois, E., *et al.*, 2012, *A&A*, 548, A40
- Cesarsky, C. J., Abergel, A., Agnese, P., *et al.*, 1996, *A&A*, 315, L32
- Cherchneff, I., & Barker, J.R., 1989, *ApJ*, 341, L21
- Cook, D.J., & Saykally, R.J., 1998, *ApJ*, 493, 793
- Cook, D.J., Schlemmer, S., Balucani, N., *et al.*, 1998, *J. Phys. Chem. A*, 102, 1465
- Cook, D.J., Schlemmer, S., Balucani, N., *et al.*, 1996, *Nature*, 380, 227
- Davico, G.E., Bierbaum, V.M., DePuy, C.H., Ellison, G.B., & Squires, R.R., 1995, *J. Amer. Chem. Soc.*, 117, 2590
- Friderichsen, A.V., Radziszewski, J.G., Nimlos, M.R., *et al.*, 2001, *J. Amer. Chem. Soc.*, 123, 1977
- Giard, M., Serra, G., Caux, E., Pajot, F., & Lamarre, J.M., 1989, *A&A*, 215, 92
- Gillett, F.C., Forrest, W.J., & Merrill, K.M., 1973, *ApJ*, 183, 87
- Joblin, C., & Tielens, A. (eds.), 2011, *PAHs and the Universe: A Symposium to Celebrate the 25th Anniversary of the PAH Hypothesis*, 46
- Jourdain de Muizon, M., Geballe, T.R., D'Hendecourt, L.B., & Baas, F., 1986, *Astrophys. J. Lett.*, 306, L105
- Kislov, V.V., Nguyen, T.L., Mebel, A.M., Lin, S.H., & Smith, S.C., 2004, *J. Chem. Phys.*, 120, 7008
- Léger, A., & Puget, J.L., 1984, *A&A*, 137, L5
- Nesbitt, D.J., & Field, R.W., 1996, *J. Phys. Chem.*, 100, 12735
- Peeters, E., Hony, S., Kerckhoven, C.V., *et al.*, 2002, *A&A*, 390, 1089
- Pino, T., Cao, A.T., Carpentier, Y., Dartois, E., D'Hendecourt, L., & Bréchnignac, P., 2008, *A&A*, 251, 393
- Puget, J.L., & Léger, A., 1989, *ARA&A*, 27, 161
- Shan, J., Sutton, M., & Lee, L.C., 1991, *ApJ*, 383, 459
- Sloan, G.C., Jura, M., Duley, W.W., *et al.*, 2007, *ApJ*, 664, 1144
- Spedding, H., & Whiffen, D.H., 1956, *Proc. Royal Soc. A*, 238, 245
- Suto, M., Wang, X., Shan, J., & Lee, L., 1992, *J. Quant. Spectr. Rad. Transfer*, 48, 79
- Tsai, S.-T., Lin, C.-K., Lee, Y. T., & Ni, C.-K., 2000, *J. Chem. Phys.*, 113, 67
- Williams, R.M., & Leone, S.R., 1995, *ApJ*, 443, 675
- Yerram, M.L., Brenner, J.D., King, K.D., & Barker, J.R., 1990, *J. Phys. Chem.*, 94, 6341